Systematic investigation of genetic vulnerabilities across cancer cell lines reveals lineage-specific dependencies in ovarian cancer

Hiu Wing Cheung[a,b,1], Glenn S. Cowley[b,1], Barbara A. Weir[b,1], Jesse S. Boehm[b,1], Scott Rusin[b], Justine A. Scott[b], Alexandra East[b], Levi D. Ali[b], Patrick H. Lizotte[b], Terence C. Wong[b], Guozhi Jiang[b], Jessica Hsiao[b], Craig H. Mermel[a,b,c], Gad Getz[b], Jordi Barretina[a,b], Shuba Gopal[b], Pablo Tamayo[b], Joshua Gould[b], Aviad Tsherniak[b], Nicolas Stransky[b], Biao Luo[b], Yin Ren[d], Ronny Drapkin[e,f], Sangeeta N. Bhatia[b,d,g,h,i], Jill P. Mesirov[b], Levi A. Garraway[a,b,c,g], Matthew Meyerson[a,b,c,e], Eric S. Lander[b,2], David E. Root[b,2], and William C. Hahn[a,b,c,g,2]

[a]Department of Medical Oncology, [c]Center for Cancer Genome Discovery and [f]Center for Molecular Oncologic Pathology, Dana-Farber Cancer Institute, Boston, MA 02115; [b]Broad Institute of Harvard and MIT, Cambridge, MA 02142; [d]Harvard-MIT Division of Health Sciences and Technology and [h]Electrical Engineering and Computer Science, David H. Koch Institute for Integrative Cancer Research, Massachusetts Institute of Technology, Cambridge, MA 02139; Departments of [e]Pathology and [g]Medicine, Brigham and Women's Hospital, Harvard Medical School, Boston, MA 02115; and [i]Howard Hughes Medical Institute, Chevy Chase, MD 20815

Contributed by Eric S. Lander, June 13, 2011 (sent for review April 13, 2011)

A comprehensive understanding of the molecular vulnerabilities of every type of cancer will provide a powerful roadmap to guide therapeutic approaches. Efforts such as The Cancer Genome Atlas Project will identify genes with aberrant copy number, sequence, or expression in various cancer types, providing a survey of the genes that may have a causal role in cancer. A complementary approach is to perform systematic loss-of-function studies to identify essential genes in particular cancer cell types. We have begun a systematic effort, termed Project Achilles, aimed at identifying genetic vulnerabilities across large numbers of cancer cell lines. Here, we report the assessment of the essentiality of 11,194 genes in 102 human cancer cell lines. We show that the integration of these functional data with information derived from surveying cancer genomes pinpoints known and previously undescribed lineage-specific dependencies across a wide spectrum of cancers. In particular, we found 54 genes that are specifically essential for the proliferation and viability of ovarian cancer cells and also amplified in primary tumors or differentially overexpressed in ovarian cancer cell lines. One such gene, *PAX8*, is focally amplified in 16% of high-grade serous ovarian cancers and expressed at higher levels in ovarian tumors. Suppression of *PAX8* selectively induces apoptotic cell death of ovarian cancer cells. These results identify *PAX8* as an ovarian lineage-specific dependency. More generally, these observations demonstrate that the integration of genome-scale functional and structural studies provides an efficient path to identify dependencies of specific cancer types on particular genes and pathways.

high throughput | RNAi | oncogene | lineage

The application of whole-genome approaches to identify genetic alterations in cancer genomes is providing new insights into the spectrum of molecular events that occur in human tumors. Although in some cases this knowledge immediately illuminates a path toward clinical implementation, the long lists of genes with aberrant sequence, copy number, or expression in tumors already found make it clear that complementary information from systematic functional studies will be essential to obtain a comprehensive molecular understanding of cancer and to convert this knowledge into therapeutic strategies.

Most ovarian cancer patients present at an advanced stage with widely disseminated disease in the peritoneal cavity. Despite advances in surgery and chemotherapy, the majority of ovarian cancer patients re-present with relapsed and progressively chemotherapy-resistant and lethal disease. The Cancer Genome Atlas (TCGA) Project has characterized nearly 500 primary high-grade serous ovarian cancer genomes to identify recurrent genetic alterations in ovarian cancer (1).

A major feature of ovarian cancers is recurrent regions of copy-number alteration (1). A small number of these recurrent genomic events harbor known oncogenes and tumor suppressor genes, such as *MYC*, *CCNE1*, and *RB* (2). However, as in other cancers, the specific genes out of the ~1,800 genes targeted by recurrent amplification events remain undefined. Here, we report a genome-scale functional study to identify genes that are essential for the survival of 102 human cancer cell lines. The interrogation of a large number of cancer cell lines provides increased power to identify relationships between gene expression and dependence. To demonstrate the utility of integrating these data with results from cancer genome characterization, we focused on ovarian cancer and identified ovarian cancer lineage-specific dependencies.

Results

To identify genes essential for the proliferation and survival of human cancer cell lines, we performed genome-scale, pooled short hairpin RNA (shRNA) screens (3) in 102 cell lines (Fig. 1*A* and Fig. S1*A*), including 25 ovarian, 18 colon, 13 pancreatic, 9 esophageal, 8 non-small-cell lung cancer (NSCLC), and 6 glioblastoma cancer cell lines (Table S1). Each cell line was infected in quadruplicate (Fig. S2*A*) with a pool of lentivirally delivered shRNAs, composed of 54,020 shRNAs targeting 11,194 genes, and propagated for at least 16 doublings. The abundance of shRNA sequences at the endpoint relative to the initial reference pool was measured by microarray hybridization. We developed a standardized analytical pipeline to assess the effects on proliferation induced by each shRNA (Figs. S1*B* and S2 *B* and *C*). Replicate infections were highly correlated (Fig. S2 *D* and *E*), and hierarchical clustering demonstrated that the replicates clustered tightly together (Fig. 1*B*). In all, we obtained 22 million individual measurements of shRNA effects on proliferation.

Author contributions: H.W.C., G.S.C., B.A.W., J.S.B., E.S.L., D.E.R., and W.C.H. designed research; H.W.C., G.S.C., B.A.W., J.S.B., S.R., J.A.S., A.E., L.D.A., P.H.L., T.C.W., G.J., and J.H. performed research; C.H.M., G.G., J.B., S.G., P.T., A.T., N.S., B.L., Y.R., R.D., S.N.B., and L.A.G. contributed new reagents/analytic tools; B.A.W., S.G., P.T., J.G., A.T., J.P.M., M.M., E.S.L., D.E.R., and W.C.H. analyzed data; and H.W.C., G.S.C., B.A.W., J.S.B., E.S.L., D.E.R., and W.C.H. wrote the paper.

Conflict of interest statement: R.D., L.A.G., M.M., and W.C.H. are consultants for Novartis Pharmaceuticals.

[1]H.W.C., G.S.C., B.A.W., and J.S.B. contributed equally to this work.

[2]To whom correspondence may be addressed. E-mail: lander@broadinstitute.org, droot@broadinstitute.org, or william_hahn@dfci.harvard.edu.

This article contains supporting information online at www.pnas.org/lookup/suppl/doi:10.1073/pnas.1109363108/-/DCSupplemental.

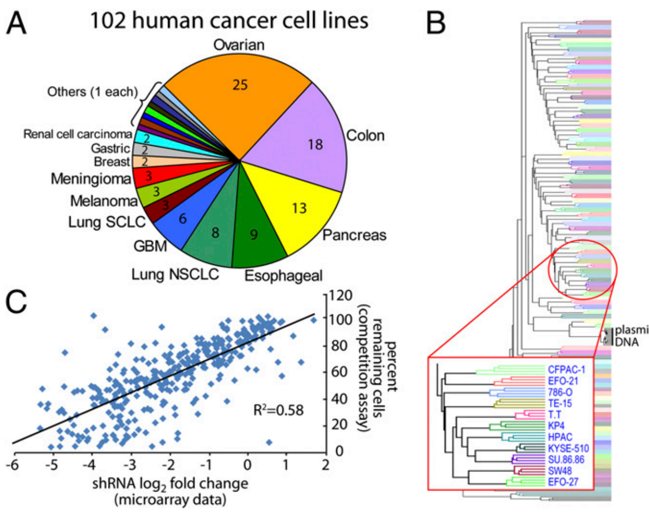

Fig. 1. Genome-scale RNAi screening identifies essential genes in 102 cancer cell lines. (*A*) Chart showing the number of cell lines from different lineages screened. (*B*) Unsupervised hierarchical clustering of the shRNA hybridization data obtained from quadruplicate screens of 102 cancer cell lines (various colors) and the shRNA plasmid DNA reference pool (15 replicates). A representative portion of the dendrogram is depicted at higher magnification. (*C*) The relative abundance 7 d after infection of OVCAR-8 cells infected with 350 individual shRNAs encoded in a GFP+ plasmid (*y* axis) correlates with the relative abundance ($\log_2$ fold change) of each shRNA measured in the pooled shRNA screen by microarray hybridization (*x* axis).

To ensure that the pooled screening process accurately measured the activity of the shRNAs, we individually retested 350 shRNAs, chosen to sample the full range of array measurements obtained in a pooled screen in OVCAR-8 cells, by performing competition assays (Fig. 1*C* and Fig. S3). Specifically, we cloned these shRNAs into a modified pLKO.1 viral vector that coexpresses GFP and used these vectors to introduce shRNAs into ~50% of an OVCAR-8 cell population. We then monitored the proportion of GFP-expressing cells over time to measure the effects of each shRNA on proliferation. The percent depletion of the shRNAs in the individual pairwise competition tests was correlated to the log(fold depletion) of these shRNA in the pooled screen (R^2 = 0.58; Fig. 1*C* and Table S2). We note that shRNAs that show the largest degree of depletion in the pooled screen exhibited more variability as would be expected at the limit of signal detection. These two correlated assessments were made at different time points, further confirming that they provide robust measures of the intrinsic proliferation effects of the individual shRNAs.

Correlation of Genetic Dependency with Properties of Cell Lines. We then sought to understand how the vulnerabilities of cancer cell lines relate to various properties, such as mutations in a specific gene, disruption of a specific pathway, or inclusion in a specific lineage. Because human cancer cell lines are genetically and epigenetically diverse, the analysis of a large number of cell lines ensures that the relationships between cell properties and the dependence of those cells on specific genes are not particular to one context. We tested whether this large dataset permits reliable inferences about the genetic vulnerability of cancers possessing specific properties. For each cell line classification, we used a class-discrimination feature selection method called the "weight of evidence" (WoE) statistic (4, 5) to rank shRNAs by their ability to distinguish the specified classes.

Dependencies of Cell Lines with Oncogenic Mutations. We first examined vulnerabilities of cell lines with *KRAS* or *BRAF* mutations. We defined "essential" genes by three complementary methods, including (*i*) WoE rank of the top shRNA targeting each gene, (*ii*) WoE rank of the top two shRNAs targeting each gene, or (*iii*) a composite score of WoE ranks for all shRNAs for each gene using the Kolmogorov–Smirnov (KS) statistic (3). The *KRAS* and *BRAF* genes themselves were ranked highly by all three methods (Fig. 2 *A* and *D*). The top scoring *KRAS*- and *BRAF*-specific shRNAs significantly discriminated between the mutant and wild-type classes (P = 1.89 × 10^{-5} and 1.89 × 10^{-4}, respectively, WoE; Fig. 2 *B* and *E*).

Interestingly, because 7/10 BRAF-mutant cell lines were derived from nonmelanoma lineages (including 5 from colon cancer), these observations suggest that cancer cell lines that harbor mutant *BRAF* exhibit a similar dependence on *BRAF*. Although initial reports suggest that clinical responses to BRAF inhibition in *BRAF*-mutant colon tumors are much less robust than those observed in *BRAF*-mutant melanomas (6), our observations indicate that *BRAF* is essential in colon cancer cell lines that express mutant *BRAF* (Fig. S4 *A* and *B*).

We next examined vulnerabilities in cell lines harboring *PIK3CA* mutations. *PIK3CA* itself strongly scored as a top differentially essential gene between *PIK3CA* mutant and *PIK3CA* wild-type cell lines in 2/3 gene-level analyses (Fig. 2 *G* and *H*). *MTOR* ranked highly in 2/3 analyses (23rd and 30th of 11,194; Fig. S4*C*); the top scoring *MTOR*-specific shRNA strongly discriminated the *PIK3CA* mutant and wild-type classes (P = 6.03 × 10^{-4}, WoE; Fig. S4*D*), indicating that cell lines that harbor *PIK3CA* mutations are also dependent on mTOR. These observations confirm prior work showing that mTOR plays an important role in PI3K signaling (7).

To assess how the number of cell lines analyzed affected these analyses, we repeated our WoE scoring of a set of shRNAs using data from smaller numbers of cell lines subsampled from the entire dataset. For the top scoring *KRAS*, *BRAF*, and *PIK3CA* shRNAs that were able to distinguish cell lines with mutant or wild-type alleles of these same respective genes, we found that the analysis of a smaller number of cell lines (<5) decreased the likelihood of discriminating between these two classes, whereas the comparison of groups composed of >10 cell lines greatly increased our ability to distinguish the two classes (Fig. 2 *C*, *F*, and *I*). We concluded that the analysis of a large number of cell lines overcomes the inherent heterogeneity of cell lines and reveals robust relationships between essentiality and particular cell features that persist across different genetic and epigenetic backgrounds. With this foundation, we undertook a preliminary exploration of what can be learned about genetic vulnerabilities of cancer cells with specific properties.

Lineage-Specific Genetic Dependencies. We hypothesized that a subset of genes showing enhanced dependencies in specific lineages would also be aberrantly activated in tumors due to amplification or overexpression. Recent studies have identified oncogenic transcription factors that are amplified, overexpressed, and essential in subsets of tumors from cancers of specific lineages, including *NKX2-1* in lung adenocarcinoma (8), *MITF* in melanoma (9), and *SOX2* in squamous cell carcinomas (10). To identify lineage-specific dependencies, we ranked shRNAs by their ability to discriminate cell lines of one lineage from cell lines from all other lineages (Fig. 3*A*). We selected the top 150 genes (1.3% of those screened) based on ranking of the top-ranked shRNAs, the top 300 genes (2.7%) by the second-best ranking shRNAs, and the top 300 genes (2.7%) as assessed by the KS statistic (ref. 3; Table S3). Three categories of essential genes were considered for further analysis: (*i*) genes scoring by all three methods from individual lineage analyses; (*ii*) genes scoring by any method that also were amplified in primary tumors (essential and amplified; Table S3); and (*iii*) genes scoring by any method that also were differentially up-regulated in cell lines derived from that lineage (essential and overexpressed; Tables S3 and S4). An overview of these results from analyses performed across six cancer lineages is displayed in Table S5.

In colon cancer cell lines, we found *KRAS*, *CTNNB1*, and *BRAF* among 23 essential genes that scored by all three methods and

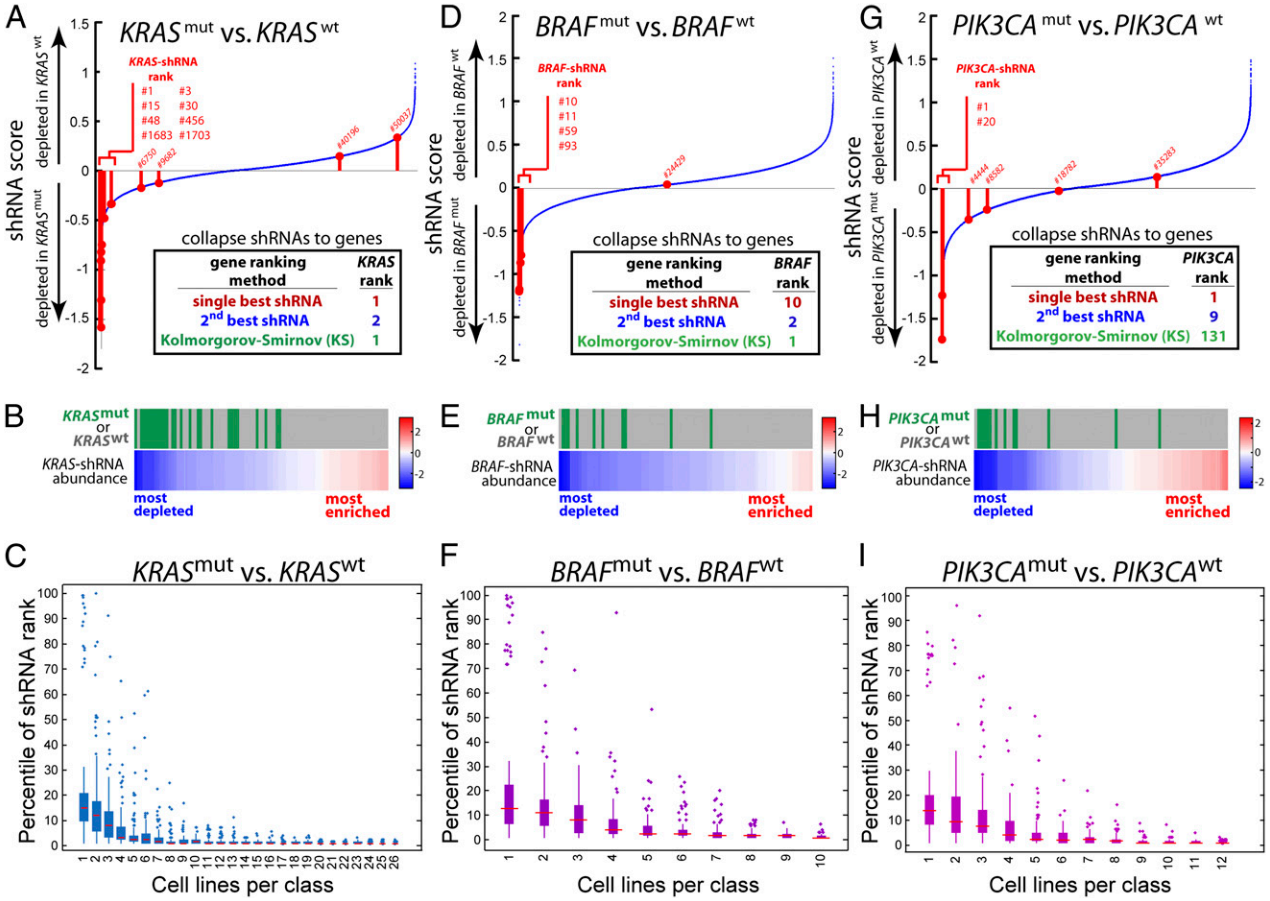

Fig. 2. Dependencies of cell lines with mutations in *KRAS*, *BRAF*, or *PIK3CA*. (*A*, *D*, and *G*) Distribution of shRNA ranks (*x* axis) by the WoE scores (*y* axis) for the class comparisons of *KRAS* mutant (mut) vs. *KRAS* wild-type (wt) cell lines (*A*), *BRAF* mutant vs. *BRAF* wt (*D*), and *PIK3CA* mutant vs. *PIK3CA* wt (*G*). shRNAs targeting *KRAS*, *BRAF*, and *PIK3CA* are highlighted in red, and their ranks are listed. *Insets* report the gene ranks of *KRAS*, *BRAF*, and *PIK3CA* for differential essentiality in the subset of cell lines with activating mutations in those respective genes. (*B*, *E*, and *H*) *KRAS* (*B*), *BRAF* (*E*), or *PIK3CA* (*H*) mutation status (mutant lines in green, wt lines in gray) correlates strongly with depletion of shRNAs targeting these genes. (*Lower*) Heatmaps report *KRAS*- (*B*), *BRAF*- (*E*), and *PIK3CA*-shRNA (*H*) fold depletion in each cell line. (*C*, *F*, and *I*) Subsets of the 102 cell lines were analyzed to assess convergence of the gene dependency results for the *KRAS* (*C*), *BRAF* (*F*), and *PIK3CA* (*I*) mutant vs. wt class comparison analyses as a function of the number of cell lines tested. Distributions of the scores of the top *KRAS*, *BRAF*, and *PIK3CA* hit shRNAs (given as the percentile of their depletion rankings, with a smaller percentage corresponding to more depleted, *y* axis) in the respective cell line class comparisons (using WoE) are shown for each of 100 trials, subsampling the indicated numbers of cell lines in each class (mutant and wt). The red bar indicates the median value for each group of subsamplings, boxes represent the 25th to 75th percentile of the data, and whiskers extend to the most extreme values of the group that are not considered outliers.

found *KRAS* and *IGF1R* (11) among 35 essential and amplified genes. In pancreatic cancer cell lines, we identified *KRAS* among 23 essential genes that scored in all three analyses (Table S5). In NSCLC, we found *NKX2-1* as the only essential gene that is both amplified and overexpressed and found *CDK6* among 7 essential and amplified genes (8). These observations provide evidence that such integrative lineage analyses identify both known oncogenes and other relevant lineage-restricted dependencies.

In addition, we identified a number of particularly interesting, previously undescribed candidate lineage-specific dependencies. For example, we found *MAP2K4*, an activator of JNK and p38 (12), among 10 genes that showed selective essentiality and expression in NSCLC. We found *MYB* (13) and *AXIN2* (14) among 9 genes that were essential and differentially expressed in colon cancer, and we identified *SOX9* (15) among 18 genes in pancreatic cancer that emerged as lineage-specific dependencies nominated by all three gene-scoring methods.

To extend these observations, we selected the ovarian lineage for deeper analysis. Of the 582 genes (5.2%) nominated as candidates for enhanced dependency in ovarian cancer cells, we identified 22 essential genes that scored in all three analytical methods (Fig. 3*B* and Table S5) and found 5 essential and overexpressed genes (Tables S4 and S5). TCGA identified 1,825 genes residing on recurrently amplified regions in ovarian tumors, and we identified 50 amplified genes as also essential (Fig. 3*B* and Table S5). The set of amplified and essential genes included the known oncogene *CCNE1* (16) and candidates including the *FRS2* adaptor protein (17), the *PRKCE* protein kinase (18), *RPTOR* (19), and the *PAX8* paired box transcription factor. Similarly to *NKX2-1* in NSCLC, *MITF* in melanoma, and *MYB* in colon cancer, *PAX8* was not only essential and amplified but also overexpressed in a lineage-specific manner.

Characterization of PAX8 Dependency in Ovarian Cancer. *PAX8* was the only gene that was (*i*) identified as an essential gene in all three scoring methods, (*ii*) amplified in primary high-grade serous ovarian tumors, and (*iii*) differentially expressed in ovarian cancer cell lines (Table S5). Cell line subsampling analysis revealed that the large number of ovarian cell lines screened enabled the identification of this previously undescribed dependency (Fig. 3*C*).

PAX8 is a lineage-restricted transcription factor that plays an essential role in organogenesis of the Müllerian system (20), the thyroid, and the kidney (21). *PAX8* was previously found to be

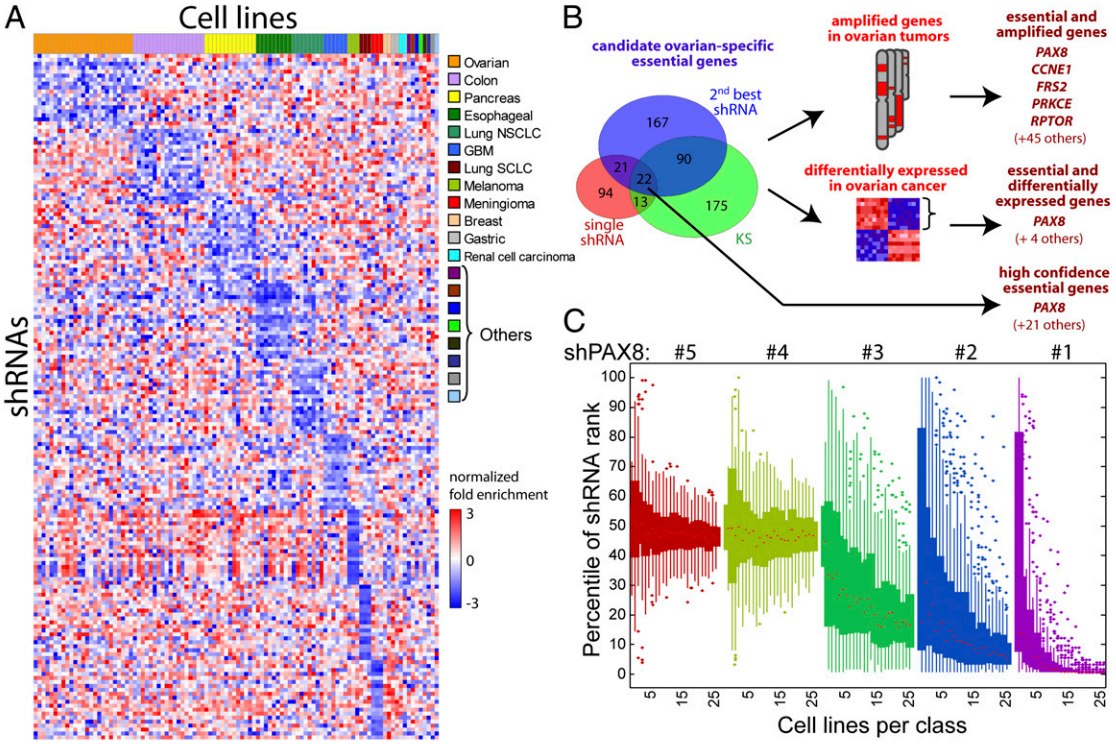

Fig. 3. Lineage-specific dependencies. (*A*) Heatmap of differentially antiproliferative shRNAs in cell lines from individual cancer lineages in comparison with all others. The top 20 shRNAs that distinguish each lineage from the others are displayed. (*B*) Ovarian-specific dependencies. Three complementary methods of gene scoring [ranking by (*i*) best or (*ii*) second best scoring shRNA or (*iii*) composite of all shRNAs for the gene using a KS statistic identified 582 (5.2%) genes that were selectively required for ovarian cancer cell proliferation. Fifty of these were among the 1,825 recurrently amplified genes in primary high-grade serous ovarian tumors (1). Among the 200 genes that were differentially overexpressed in ovarian cancer cell lines, 114 genes were included in the shRNA pool, and 5 genes showed enhanced essentiality in ovarian cancer lines. Twenty-two of these genes that were scored by all three gene-scoring methods were considered as high-confidence essential genes. (*C*) Distributions of the scores of *PAX8* shRNA (given as the percentile of their rankings, *y* axis) after 100 trials of the ovarian vs. nonovarian WoE comparison, for equal class sizes of 1–25 (*x* axis; colors indicate *PAX8* shRNAs 1–5). The red bar indicates the median value for each group of subsamplings, boxes represent the 25th to 75th percentile of the data, and whiskers extend to the most extreme values of the group that are not considered outliers.

overexpressed in ovarian cancers (22) and implicated in follicular thyroid cancer development (23). We observed that *PAX8* was the most differentially expressed gene when we compared ovarian cell lines to all of the other cancer cell lines (Fig. 4*A*). Furthermore, we found that *PAX8* was amplified in 16% of primary ovarian tumors [$\log_2$(copy number ratio) > 0.3; $n = 345$] in a peak (2q13) that also contains *PSD4* and *LOC654433* (Fig. 4*B*).

We further examined the relationships among *PAX8* amplification, *PAX8* expression, and dependence on *PAX8* in ovarian cancer cells. The *PAX8*-specific shRNA that scored 7th out of 54,020 shRNAs and the 2nd-ranking *PAX8* shRNA both suppressed PAX8 (Fig. S4*E*). The sensitivity of cell lines to inhibition by the highest ranked *PAX8*-specific shRNA correlated with the level of *PAX8* expression, based on comparison of cell lines with high vs. low *PAX8* levels ($P = 2.14 \times 10^{-8}$, *t* test; Fig. 4*C*). Cell lines expressing high levels of *PAX8* included the vast majority (21/25) of ovarian cancer cell lines as well as a renal and an endometrial cancer line. These observations suggested that the expression of *PAX8* is selectively required for the proliferation/survival of cell lines expressing *PAX8*.

To confirm these findings, we introduced two distinct shRNAs targeting *PAX8* into 17 cell lines. We found that suppression of *PAX8* resulted in a >50% reduction in the viability in six of eight ovarian cancer cell lines (Fig. 4*D*), but failed to affect the proliferation of immortalized human ovarian surface epithelial cells (IOSE-T80; ref. 24) and eight other cell lines that did not express PAX8 (Fig. 4*E*). The six sensitive ovarian cell lines included three cell lines with amplification of 2q13 in which the *PAX8* locus resides (Fig. S4*F*) and three additional cell lines that express higher levels of PAX8 protein compared with IOSE-T80 cells (Fig. 4*D*). Suppression of *PAX8* induced apoptosis in these ovarian cancer cell lines (Fig. 4*F*). In contrast, the two cell lines (COV504 and OV-90) least sensitive to *PAX8* suppression did not harbor the 2q13 amplification and expressed relatively low levels of PAX8 (Fig. 4*D*). These observations suggest that *PAX8* represents a lineage-specific essential gene in a significant subset of ovarian cancer.

Discussion

The integrated analysis of functional dependencies and alterations in cancer genomes presented herein identified potential targets in ovarian, lung, colon, glioblastoma, pancreatic, and esophageal cancers. Among these candidate genes, we identified known oncogenes and lineage-specific dependencies as well as previously undescribed candidates, including the *PAX8* transcription factor in ovarian cancer. Although shRNA screens performed in small numbers of cell lines have identified essential genes in specific contexts, the interrogation of genes across a large number of human cancer cell lines through Project Achilles provides a substantially more robust assessment of gene dependence and overcomes confounding effects due to the inherent heterogeneity of human cancer cell lines. These datasets will enable a wide range of analyses to connect particular cancer genotypes to dependencies.

As an initial approach, we elected to explore dependencies harbored by a majority of ovarian cancers. We pinpointed 5 genes displaying enhanced essentiality in ovarian cancer and differential overexpression in ovarian cell lines and 50 genes displaying enhanced essentiality in ovarian cancer and amplification in ovarian tumors. Further studies will be necessary to

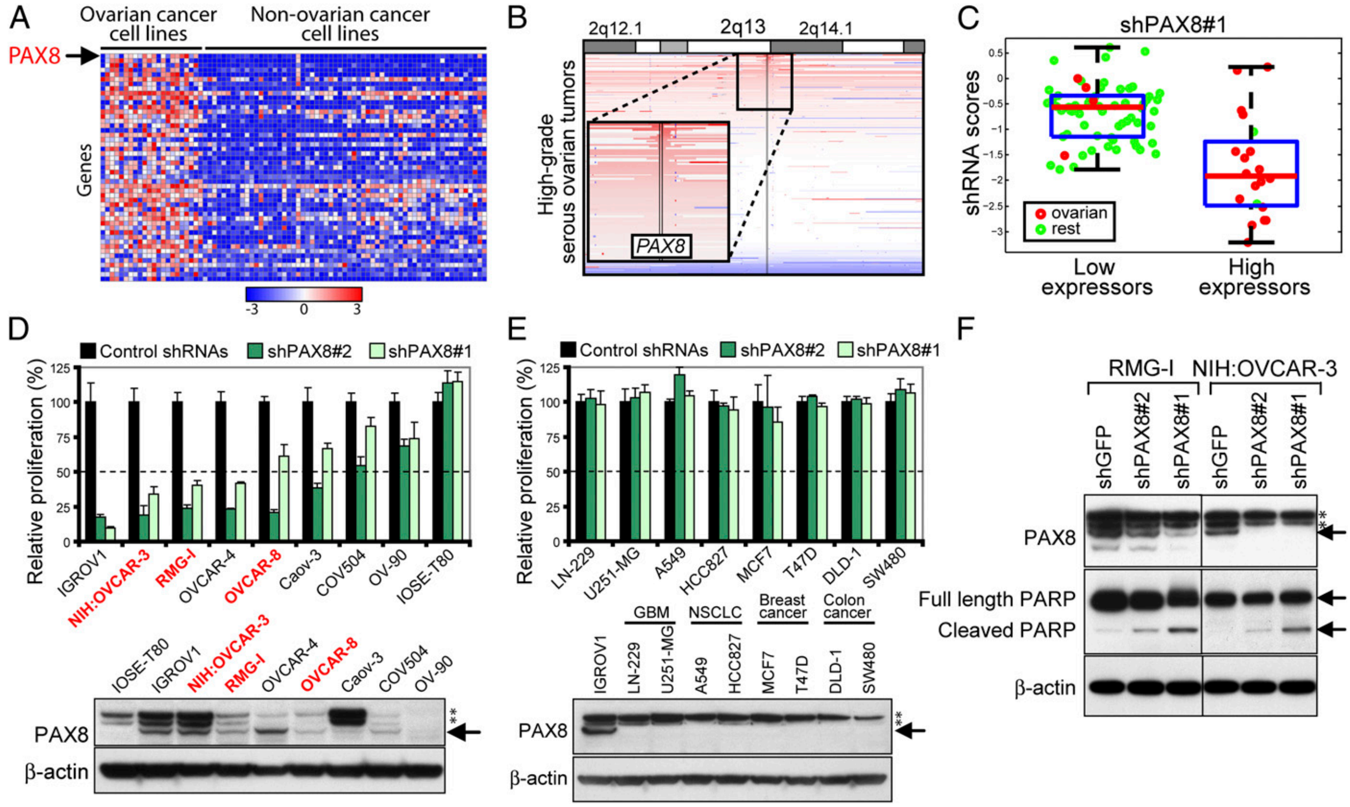

Fig. 4. *PAX8* is essential for ovarian cancer cell proliferation and survival. (*A*) *PAX8* is the top-ranked differentially expressed gene between ovarian and nonovarian cancer cell lines. Arrow indicates *PAX8*. (*B*) SNP array colorgrams depict genomic amplification of *PAX8* in primary high-grade serous ovarian cancers (1). Regions of genomic amplification and deletion are denoted in red and blue, respectively. SNP array profiles derived from primary ovarian tumors were sorted based on the degree of amplification of each gene. Black vertical lines denote the boundaries of the *PAX8* gene. (*C*) Boxplot showing significant difference in the degree of depletion of a *PAX8*-specific shRNA in 63 cell lines with low levels of *PAX8* compared with 20 lines with high levels of *PAX8* ($P = 2.14 \times 10^{-8}$, *t* test). Cell lines were divided into high- and low-expressing groups. The red line indicates the median value for each group, boxes represent the 25th to 75th percentile of the data, and whiskers extend to the most extreme values of the group that are not considered outliers. Ovarian cancer cell lines are plotted with red circles; cell lines from all other lineages are plotted with green circles. (*D Upper*) Effects of *PAX8* suppression on proliferation in eight ovarian cancer cell lines; dotted line indicates 50% relative proliferation. (*Lower*) Immunoblot of PAX8 in a panel of eight ovarian cancer cell lines and in immortalized IOSE-T80 cells. Cell lines with amplification of 2q13 ($\log_2$ copy number ratio > 0.3) are marked in red. * denotes nonspecific band. (*E Upper*) Effects of *PAX8* suppression on proliferation of cell lines from indicated cancer types. (*Lower*) Immunoblot of PAX8. Error bars indicate SD of six replicate measurements. (*F*) Immunoblot of poly(ADP-ribose) polymerase after *PAX8* suppression in two 2q13-amplified cell lines. * denotes nonspecific band.

extend the preliminary findings for these ovarian cancer dependencies. A single gene, *PAX8*, emerged from every one of these analyses. Our subsequent experiments confirmed *PAX8* to be a lineage-specific survival gene that is essential for proliferation of ovarian cancer cells, highly expressed in ovarian cancer lines, and amplified in a substantial fraction of primary ovarian tumors.

PAX8 has been shown to play an essential role in the normal development of the thyroid gland (21) and female genital tract (20). The thyroid gland in *Pax8*-deficient mice is completely devoid of thyroid hormone-producing follicular cells and exhibits severe growth retardation within a week after birth (21). Thyroxine substitution enables *Pax8*-deficient mice to survive to adulthood (20). However, these mice are infertile because of the absence of uterus and vaginal openings (20), indicating that *Pax8* is also essential for the development of the Müllerian duct. In the reproductive tract, PAX8 expression is restricted to secretory cells of the fallopian tube epithelium (22), which recent reports suggest represent a cell of origin for serous ovarian cancer (25). These findings suggest that *PAX8* plays critical roles both in normal development of female genital tract and in high-grade serous ovarian tumors.

A number of genes involved in the differentiation programs for specific tissue lineages are amplified in cancers that arise from these tissues. For example, *NKX2-1* (8), *MITF* (9), and *SOX2* (10) are amplified and essential for the survival of significant subsets of NSCLC, melanoma, and squamous cell carcinomas, respectively. Our results show that *PAX8* belongs to this distinct class of lineage-survival genes that are required for both normal development of specific tissues and for cancer cell proliferation/survival. Although different subtypes of ovarian cancer are likely to harbor distinct profiles of genetic alterations (2), our findings suggest that for most ovarian cancer cell lines, *PAX8*-driven transcription programs transiently active during normal development are coopted to maintain the malignant state.

Epithelial ovarian cancers have been classified into four major subtypes based on histology: serous, clear cell, endometrioid, and mucinous (2). These major subtypes show morphologic features that resemble those of the epithelia of the reproductive tract derived from the Müllerian duct (2). Previous studies using immunohistochemistry showed that 89–100% of serous, clear cell, and endometrioid subtypes and 8% of mucinous subtype express PAX8 (26). The majority of the ovarian cancer cell lines that we screened (20/25) belong to the serous subtype or had a mixed morphology. A larger collection of cancer cell lines will facilitate a deeper investigation of ovarian cancer subtypes.

Given the genetic heterogeneity of cancer, screening large numbers of cell lines is required to have sufficient statistical power to extract known and novel relationships and provide adequate representation of individual sublineage classes. Although the classification of cell lines based on a single characteristic is unlikely to segregate cell lines into homogenous groups, our observations indicate that by including many cell line representatives of each class of interest, it is still possible to discover underlying relationships between genotype or lineage and essential genes. Integration of these data with information from the analyses of structural alterations in cancer genomes will further facilitate the systematic identification of genes critical to oncogenesis.

The approach described here can be extended to enable systematic interrogation of codependences beyond those analyzed here, including synthetic lethal relationships with activated oncogenes or inactivated tumor suppressor genes (27). Analyses of dependencies of cell lines with particular characteristics have the potential to discover novel targets, for example, by integrating the output of these types of screens with information emerging from the cataloging of mutations and other alterations in cancer genomes.

More generally, as large-scale efforts to characterize cancer genomes accelerate, these observations illustrate a path to functionally characterize the genes found to be altered in tumors and to identify the subset of such genes critical to cancer initiation and maintenance. To this end, we have made this dataset available (www.broadinstitute.org/igp) and will update the Project Achilles database as more data are obtained. Beyond the specific findings reported herein, we anticipate that this dataset will prove useful to identify correlations between genetic features and essential genes in human cancer cell lines.

Materials and Methods

Pooled shRNA Screening. Lentiviral pLKO.1- shRNA constructs were obtained from the RNAi Consortium, and the human 54K pool of 54,020 shRNA plasmids was assembled by combining 16 normalized subpools of ~3400 shRNA plasmids. The list of 54,020 shRNAs can be found at http://www.broadinstitute.org/igp. Genome-scale pooled shRNA screens to identify genes essential for proliferation in 102 cancer cell lines were performed (3) using a lentivirally delivered pool of 54,020 shRNAs targeting 11,194 genes. The culture conditions for all cancer cell lines are listed in Table S1. Each cell line was infected in quadruplicate and propagated for at least 16 population doublings. The abundance of shRNA constructs relative to the initial DNA plasmid pool was measured by microarray hybridization (3) and analyzed by using a uniform pipeline. Detailed descriptions of each procedure can be found in *SI Methods*.

Data Processing, Class Comparison, and Gene Ranking. Raw .CEL files from custom Affymetrix barcode arrays were processed with a modified version of dCHIP software (3). The GenePattern modules shRNAscores and NormalizeCellLines were used to calculate the log fold change in shRNA abundances for each cell line at the conclusion of the screening relative to the initial plasmid DNA reference pool and to normalize these depletion values by using peak median absolute deviation normalization, a variation of *Z* score with median absolute deviation (3). Class definition files (.cls) were made by using the GenePattern module SubsetGctandCls; definitions included cell line lineage (e.g., ovarian cancer, NSCLC, etc.) or genetic alterations (28, 29). To compute the statistical evidence that a given shRNA contributes to the observed essentiality phenotype between two classes of interest, we used a WoE approach (4, 5). The GENE-E program (http://www.broadinstitute.org/cancer/software/GENE-E; ref. 3) was used to collapse shRNAscores to gene rankings by three complementary methods. These methods included (*i*) ranking genes by their highest shRNA depletion score, (*ii*) ranking genes based on the *P* value rank (correcting for different set sizes of shRNA targeting different genes) of their second best ranked shRNA, and (*iii*) ranking genes using a KS statistic in an approach similar to gene set enrichment analysis (RNAi gene enrichment ranking; ref. 3). Detailed descriptions of each procedure can be found in *SI Methods*. All data files, accessory files, and GenePattern modules can be found through the Integrative Genomics Portal (http://www.broadinstitute.org/igp).

Competition Assay. OVCAR-8 (5×10^4) cells were seeded into each well of a 96-well plate and spin-infected with 2 or 4 μL of lentiviruses (in duplicate) at 930 × *g* for 2 h at 30 °C in the presence of 4 μg/mL polybrene to transduce ~50% of the cells. Cells were then trypsinized and replated into 24-well plates. The percent of GFP+ cells at 3 and 7 d after infection was measured using BD LSR II flow cytometry system equipped with a high-throughput sampler (BD Biosciences). The fraction of GFP+ cells 7 d after infection relative to 3 d after infection was calculated. Data represent mean ± SD of duplicate infections.

ACKNOWLEDGMENTS. We thank M. Reich, A. Derr, and T. Liefield for assistance with analysis and data portal creation. This work was supported in part by National Institutes of Health Grants R33 CA128625, U54 CA112962, and RC2 CA148268, Novartis Pharmaceuticals, Richard Hunt, and the H. L. Snyder Foundation.

1. TCGA-Network (2011) Integrated genomic analyses of ovarian carcinoma. *Nature* 474: 609–615.
2. Bast RC, Jr., Hennessy B, Mills GB (2009) The biology of ovarian cancer: New opportunities for translation. *Nat Rev Cancer* 9:415–428.
3. Luo B, et al. (2008) Highly parallel identification of essential genes in cancer cells. *Proc Natl Acad Sci USA* 105:20380–20385.
4. Good IJ (1983) *Good Thinking: The Foundations of Probability and Its Applications* (University of Minnesota Press, Minneapolis).
5. Tamayo P, et al. (2011) Predicting relapse in patients with medulloblastoma by integrating evidence from clinical and genomic features. *J Clin Oncol* 29:1415–1423.
6. Flaherty KT, et al. (2010) Inhibition of mutated, activated BRAF in metastatic melanoma. *N Engl J Med* 363:809–819.
7. Weigelt B, Warne PH, Downward J (2011) PIK3CA mutation, but not PTEN loss of function, determines the sensitivity of breast cancer cells to mTOR inhibitory drugs. *Oncogene*, in press.
8. Weir BA, et al. (2007) Characterizing the cancer genome in lung adenocarcinoma. *Nature* 450:893–898.
9. Garraway LA, et al. (2005) Integrative genomic analyses identify MITF as a lineage survival oncogene amplified in malignant melanoma. *Nature* 436:117–122.
10. Bass AJ, et al. (2009) SOX2 is an amplified lineage-survival oncogene in lung and esophageal squamous cell carcinomas. *Nat Genet* 41:1238–1242.
11. Lopez T, Hanahan D (2002) Elevated levels of IGF-1 receptor convey invasive and metastatic capability in a mouse model of pancreatic islet tumorigenesis. *Cancer Cell* 1:339–353.
12. Khatlani TS, et al. (2007) c-Jun N-terminal kinase is activated in non-small-cell lung cancer and promotes neoplastic transformation in human bronchial epithelial cells. *Oncogene* 26:2658–2666.
13. Ramsay RG, Gonda TJ (2008) MYB function in normal and cancer cells. *Nat Rev Cancer* 8:523–534.
14. Lammi L, et al. (2004) Mutations in AXIN2 cause familial tooth agenesis and predispose to colorectal cancer. *Am J Hum Genet* 74:1043–1050.
15. Lynn FC, et al. (2007) Sox9 coordinates a transcriptional network in pancreatic progenitor cells. *Proc Natl Acad Sci USA* 104:10500–10505.
16. Etemadmoghadam D, et al.; Australian Ovarian Cancer Study Group (2010) Amplicon-dependent CCNE1 expression is critical for clonogenic survival after cisplatin treatment and is correlated with 20q11 gain in ovarian cancer. *PLoS ONE* 5:e15498.
17. Gotoh N (2008) Regulation of growth factor signaling by FRS2 family docking/scaffold adaptor proteins. *Cancer Sci* 99:1319–1325.
18. Okhrimenko H, et al. (2005) Protein kinase C-epsilon regulates the apoptosis and survival of glioma cells. *Cancer Res* 65:7301–7309.
19. Kim DH, Sabatini DM (2004) Raptor and mTOR: Subunits of a nutrient-sensitive complex. *Curr Top Microbiol Immunol* 279:259–270.
20. Mittag J, Winterhager E, Bauer K, Grümmer R (2007) Congenital hypothyroid female *pax8*-deficient mice are infertile despite thyroid hormone replacement therapy. *Endocrinology* 148:719–725.
21. Mansouri A, Chowdhury K, Gruss P (1998) Follicular cells of the thyroid gland require *Pax8* gene function. *Nat Genet* 19:87–90.
22. Bowen NJ, et al. (2007) Emerging roles for PAX8 in ovarian cancer and endosalpingeal development. *Gynecol Oncol* 104:331–337.
23. Wang Q, et al. (2008) Pax genes in embryogenesis and oncogenesis. *J Cell Mol Med* 12 (6A):2281–2294.
24. Liu J, et al. (2004) A genetically defined model for human ovarian cancer. *Cancer Res* 64:1655–1663.
25. Carlson JW, et al. (2008) Serous tubal intraepithelial carcinoma: Its potential role in primary peritoneal serous carcinoma and serous cancer prevention. *J Clin Oncol* 26: 4160–4165.
26. Köbel M, et al. (2008) Ovarian carcinoma subtypes are different diseases: Implications for biomarker studies. *PLoS Med* 5:e232.
27. Kaelin WG, Jr. (2009) Synthetic lethality: A framework for the development of wiser cancer therapeutics. *Genome Med* 1:99.
28. Thomas RK, et al. (2007) High-throughput oncogene mutation profiling in human cancer. *Nat Genet* 39:347–351.
29. Forbes SA, et al. (2008) The Catalogue of Somatic Mutations in Cancer (COSMIC). *Curr Protoc Hum Genet* 57:10.11.1–10.11.26.

Supporting Information

Cheung et al. 10.1073/pnas.1109363108

SI Materials and Methods

Cell Culture and Fingerprinting of Cell Lines. The culture conditions for all cancer cell lines are listed in Table S1. To verify the identity of each cell line, Sequenom genotyping assays for a panel of 48 SNP loci were performed on genomic DNA isolated from each replicate of cell lines at the conclusion of the screen at the Broad Institute Genetic Analysis Platform. A reference "fingerprint" containing 33 of these loci for each cell line was derived from Affymetrix 6.0 array data (http://www.broadinstitute.org/ccle) or prescreen Sequenom genotyping.

Construction of Pooled shRNA Library. The human 54K pool of 54,020 shRNA plasmids from the RNAi Consortium was assembled by combining 16 normalized subpools of ~3,400 shRNA plasmids each. Each subpool was used to transform ElectroMAX DH5α-E cells (Invitrogen) by electroporation and plated onto five 24 × 24-cm^2 bioassay dishes (Nunc). DNA was purified from the plated transformants by using a HiSpeed Plasmid Maxi Kit (Qiagen). These subpools were then combined to create the 54K shRNA pool. Then, 2 μg of this pool was used to transform DH5α cells and plated onto 50 24 × 24-cm^2 bioassay dishes. DNA was purified from the plated transformants and used for virus production. A complete list of shRNAs along with unique TRCN identifiers is publicly available (http://www.broadinstitute.org/rnai/public/).

Virus Pool Production, Infection, and Cell Propagation. Production of lentivirus from the 54K shRNA pool was performed as described (1). A single batch of ~5 L of virus was aliquoted and frozen at −80 °C for all infections.

Infections were performed as described (1) with the following modifications. To determine viral volume that would produce a multiplicity of infection (MOI) of 0.3–0.5 for each cell line, cells were infected with a titration of six different volumes (0–400 μL) of virus and cultured in the presence or absence of puromycin. Before large-scale infection, cells were filtered through a 40-μm cell strainer (BD Falcon). For each of the quadruplicate infections, 3.7×10^7 cells were resuspended in 24 mL of medium containing 4 μg/mL polybrene, and the appropriate volume of 54K library lentiviruses was added. This mixture was seeded into a 12-well plate at ~2 mL per well. A spin infection was performed by centrifugation at 930 × *g* for 2 h at 30 °C.

For suspension cells, supernatants were gently aspirated off after infection, and fresh medium was added to the 12-well plates. After 20 h, the 12 wells from each replicate infection were pooled, and the combined cells were transferred into a T175-flask containing 200 mL of medium containing puromycin. At 4 d after selection, for each of the four replicates, 2×10^7 cells were plated into a new T175-flask and cultured in 200 mL of medium containing puromycin. For all subsequent passages, 1.1×10^7 cells per replicate were carried over. The remaining cells for all passages were collected, resuspended in 1 mL of PBS, and stored at −20 °C for genomic DNA isolation.

For adherent cells, supernatants were gently aspirated off after spin infection, and fresh medium was added to the 12-well plates. After 20 h the 12 wells from each replicate were trypsinized, and cells combined and plated in two T225-flasks containing 60 mL of medium containing puromycin. Passaging for each cell line was continued for at least 16 population doublings or 28 d, whichever was longer. Puromycin selection was maintained for the entire experiment.

In-Line Infection Calculation. At 20 h after large-scale infection, a small fraction of cells ($1.5–3 \times 10^5$) from each replicate were plated into each well of six-well plates in the presence or absence of puromycin. Control wells with 100% uninfected cells were included to verify complete puromycin killing of uninfected cells. Ninety-six hours later, viable cells were counted using trypan blue staining. The infection rate was determined by calculating the number of viable cells selected in puromycin divided by the number of viable cells without puromycin selection. Screening continued only when the infection rates were within the range of 30–65% to provide an MOI = 1 and to yield a sufficient number of cells to provide adequate shRNA representation.

Genomic DNA Isolation and Array Hybridization. Genomic DNA isolation, half-hairpin barcode production, and array hybridization were performed as described (1). For PCR amplification of shRNA sequences, minimum of 50 μg of genomic DNA was used as template for each replicate. Therefore, multiple PCR reactions were performed, each using 3 μg of genomic DNA per 50 μL reaction volume.

Quality Control of Hybridization. Scans of each array were visually inspected to detect spatial irregularities or hybridization profiles with signal out of the linear range. Such aberrant array hybridization data were discarded. Interreplicate agreement for experimental replicates of each cell line was assessed from their MvA plots using the GenePattern module MvAplots, which defines the interquartile range (IQR) value for each pairwise comparison of replicates of a cell line. Replicate pairs that have a calculated IQR value of <1.2 were retained for analysis. To confirm that experimental replicates derived from the same cell line exhibited very small discrepancies compared with intercell line differences, we performed unsupervised hierarchical clustering with a Pearson correlation. Replicates that failed to tightly cluster with each other were discarded. The arrays were also filtered based on the relative difference between the distribution of human and mouse probes in the raw data for each array. Arrays with <30% of human probes with signal above the mouse probe signal were removed. Any line with less than three replicates passing any QC measure was also removed.

Data Preprocessing for Custom TRC shRNA Arrays. Raw .CEL files from custom Affymetrix barcode arrays were processed with a modified version of dCHIP software (1). "Barcode" array type, "average" model method, and fifth percentile of region (PM-only) background selection were used as parameters. "Running median" and "All probes" were chosen as parameters for normalization, and data were logged before further analysis.

shRNA Scoring. After data preprocessing, the GenePattern modules "RNAigctconverter" and "MakeArrayInfo" were used to convert preprocessed data into a .gct file and make a file of array annotations, respectively. Then the module "shRNAscores" was used to collapse values derived from replicate measurements of the abundance of each shRNA in the initial DNA pool in comparison with its abundance at the completion of replicate experiments performed on each cell line using an adjusted log fold change score. The log fold change score is the difference in means between replicates of the cell line of interest and replicates of the initial DNA pool. This score was adjusted to deemphasize shRNAs that showed high variability among replicates of the DNA pool, which likely arises from technical artifacts including shRNA underrepresentation in the initial

DNA pool or suboptimal array probe performance. To penalize these variable scores, we divided the log fold change score by the SD of the DNA pool after it had been mean centered at 1 and floored at 1. The log fold change scores of the least variable shRNAs from reference measurements were unaltered and the scores of the most variable shRNAs were penalized proportional to the SD of their replicate measurements from the reference pool. This adjusted log fold change score was used for subsequent processing.

Scaling and Centering Data Ranges. To normalize the shRNA depletion values between cell lines, the distribution of adjusted log fold change scores of each line was scaled and centered with peak median absolute deviation (PMAD) normalization, a variation of *Z* score with median absolute deviation (1), using the GenePattern module "NormalizeCellLines." PMAD normalization first centers the shRNAscores per cell line at 0, by subtracting the value of each shRNA from the modeled peak value of the distribution of each cell line. The peak value was obtained by taking the maximum value of the Gaussian smoothed, kernel density estimate of the distribution. The shRNAscores for each cell line were then rescaled so that each line had similar data ranges by dividing the centered data for each shRNA by the median absolute deviation (MAD) of the shRNAs for each cell line.

Class Definitions. Comparisons of PMAD normalized shRNA relative abundance data were based on behavior of shRNAs within a class or differential behavior of shRNAs between classes of cell lines. Class definitions used included cell line lineage (e.g., ovarian cancer, NSCLC, etc.) or genetic alterations (*KRAS*, *BRAF*, or *PIK3CA* mutation) (2, 3). Class definition files (.cls) were made using the GenePattern module "SubsetGctandCls."

Scoring shRNAs by Class Comparisons. To compute the statistical evidence that a given shRNA contributes to the observed essentiality phenotype between two classes of interest, we used a weight of evidence (WoE) approach. This approach computes the likelihood that a given shRNA has the ability to discriminate between the two classes of interest in a statistically significant manner. Weights of evidence scores for a particular class comparison, as defined by a class definition file, were calculated using the GenePattern module "ScorebyClassComp." The probability that any given shRNA can provide this discrimination is inferred from its posterior log-odds ratio:

$$\mathrm{Ev}(r|x) = \log\frac{P(r=\mathrm{ClassA}|x=X_i)/P(r=\mathrm{ClassB}|x=X_i)}{P(r=\mathrm{ClassA})/P(r=\mathrm{ClassB})}, \quad [1]$$

where *r* is a binary variable and is either ClassA or ClassB, *x* is a single shRNA measurement, and X_i is the shRNA level score for that shRNA.

The total evidence that the shRNA level scores provide can be computed as the average absolute evidence (AvEv):

$$\mathrm{AvEv}(\mathrm{r}|x) = \sum_{i}^{k} P(x=X_i)|\mathrm{Ev}(r|x=X_i)|, \quad [2]$$

where the sum is over all of the *k* distinct shRNAscores X_i.

To compute the conditional probabilities, we used a logistic regression model because the set of X_i shRNA level measurements is a continuous distribution. The logistic regression model that approximates the conditional probability is:

$$P(r|x) = \frac{1}{1+e^{-(A+Bx)}}. \quad [3]$$

A generalized linear model fit identified the values of the coefficients A and B so as to be able to compute the conditional probabilities in each cell line in each class. Because our primary focus was to identify shRNAs that were depleted in abundance, we ranked AvEv scores by their effects from most negative to most positive. Therefore, we used a signed AvEv from the value of coefficient B (sign(*B*)AvEv), preferentially ranking shRNAs from the most negative to the most positive WoE. In this manner, we identified shRNAs with the most discriminatory power among two classes as well as the shRNAs that were depleted in the particular class of interest (e.g., *KRAS* mutant). One advantage of this approach is that it does not assume that the shRNAscores are normally distributed within each class, an assumption that is central to other metrics of differential assessment including *t* tests and signal-to-noise ratios.

Data Files and GenePattern Modules. A portal with data files, accessory files, and GenePattern modules for reproducing the analysis to produce shRNAscores can be found on the Integrative Genomics portal (http://www.broadinstitute.org/IGP). Ranked shRNA and gene lists for all of the analyses presented in this paper can also be found there.

Subsampling Analysis. A group of 124 shRNAs, including control shRNAs and shRNAs targeting *KRAS*, *BRAF*, *PIK3CA*, and *PAX8,* as well as other genes, were used for an analysis of class size. WoE comparisons of *KRAS* mutant vs. WT, *BRAF* mutant vs. WT, *PIK3CA* mutant vs. WT, and ovarian vs. non-ovarian lines were performed for these shRNAs. Every comparison was performed on 100 random subsets of cell lines taken from each class, for a range of equal class sizes (1 vs. 1, 2 vs. 2, etc.) from 1 to number of cell lines screened in each target class (1–26 for *KRAS*, 1–10 for *BRAF*, 1–12 for *PIK3CA*, and 1–25 for Ovarian). Percentile of shRNA rank (shRNA rank divided by the total number of tested shRNAs, multiplied by 100) for shRNAs specific for *KRAS* (TRCN0000033262), *BRAF* (TRCN0000006291), *PIK3CA* (TRCN0000039607), and *PAX8* (see *Plasmids*) from the *KRAS*, *BRAF*, *PIK3CA*, and ovarian subsampled comparisons, respectively, were plotted as grouped boxplots by target class size.

Collapsing shRNAScores to Gene Rankings. The GENE-E program (http://www.broadinstitute.org/cancer/software/GENE-E) (1) was used to collapse shRNA differential essentiality scores to gene rankings by three complementary methods. These methods included (*i*) ranking genes by their highest shRNA depletion score, (*ii*) ranking genes based on the *P* value rank of their second best ranked shRNA, and (*iii*) ranking genes using a KS statistic in an approach similar to gene set enrichment analysis (RNAi gene enrichment ranking) for scoring genes based on the *P* value rank of the normalized enrichment scores (NES; ref. 1). The NES represents the bias of the set of shRNAs targeting each gene toward the phenotype of interest, for example, depletion in *KRAS* mutant lines.

The majority of the 11,194 genes were represented by 5 shRNAs (range 2–31 shRNAs per gene, excluding control shRNAs). Out of the initial 54,020 shRNAs in the pool, 979 shRNAs were excluded from the gene rankings because they contained overlapping sequence (offset of less than 3 base pairs) with another shRNA construct for the same gene. Nine additional shRNAs, representing 9 genes, were removed automatically by GENE-E, before gene ranking analysis. Control shRNAs target GFP, RFP, Luciferase, and LacZ, and each control shRNA is represented as 5 replicate measurements on the microarray.

To assess the significance of a gene score obtained by the second best or KS scoring methods described, *P* values were computed based on 10,000 random samplings of shRNAs to create artificial genes with the same number of shRNAs as the gene of interest (correcting for different set sizes of shRNA targeting different genes). The *P* value reflects the number of times such an artificially constructed gene received a score as good as or better than the gene of interest. Therefore, the smaller the *P* value, the less likely such a gene score could have been obtained at random.

On average, 58% of the shRNA suppress the given target >70% using qPCR measurements of endogenous transcript levels (The RNAi Consortium); thus, a simple average of shRNAscores is not ideal because not all shRNAs are effective. Because the single shRNA and second best shRNA methods depend only on the 1–2 shRNAs of strongest effect, the influence of ineffective shRNAs on gene scores is minimized. The KS statistic however considers all shRNAs from each gene in producing a gene score. It is thus more sensitive to cases for example in which all five shRNAs score moderately for depletion. Because a higher false positive rate with the single shRNA ranking method is predicted due to off-target effects, only the top 150 genes identified by this method were selected for further analysis, whereas the top 300 genes from each of the other two methods were selected. A union was taken of the genes identified by these three methods.

Competition Assay. Of the 350 shRNA retested, 238 shRNAs were selected to represent a range of fold depletion in OVCAR-8 and OVCAR-4 cells, including shRNAs ranking from #1–19, #101–120, #501–525, #1,001–1,025, #5,001–5,025, #10,001–10,025, and #20,001–20,020). In addition, 112 shRNAs targeting 25 oncogenes or control genes were included. The 350 shRNAs are listed in Table S2. OVCAR-8 (5×10^4) cells were seeded into each well of a 96-well plate and spin-infected with 2 or 4 μL of lentiviruses (in duplicate) at 930 × *g* for 2 h at 30 °C in the presence of 4 μg/mL polybrene to transduce ~50% of the cells. Cells were then trypsinized and replated into 24-well plates. The percent of GFP+ cells at 3 and 7 d postinfection was measured using BD LSR II flow cytometry system equipped with a high-throughput sampler (BD Biosciences). The fraction of GFP+ cells 7 d postinfection relative to 3 d postinfection was calculated. Data represent mean ± SD of duplicate infections.

Analysis of Primary Tumor Data. Regions of copy number amplification identified by Genomic Identification of Significant Targets in Cancer analyses were used from publications focused on various tumor lineages, including ovarian (4), NSCLC/lung adenocarcinoma (5), glioblastoma (6), colorectal, and esophageal squamous cancers (7). When necessary, coordinates were changed to hg18. Regions in the colon and esophageal squamous lineages were manually reviewed for segmentation artifacts; potential artifacts were removed. For all lineages, all RefSeq genes within the regions of amplification were identified and cross referenced with genes interrogated in the screening library. All primary high-grade serous ovarian cancer data were downloaded from the TCGA portal (http://tcga-data.nci.nih.gov/tcga). The frequency of amplification for *PAX8* genes was determined by using a threshold of $\log_2$ copy number ratio > 0.3 within a subset of tumors in TCGA project (345 tumors). Screenshots of the same tumor data were taken using the Integrative Genome Viewer (http://www.broadinstitute.org/igv).

Differential Expression Analysis. Expression analyses were performed on cell lines with gene expression data available (*n* = 83; http://www.broadinstitute.org/ccle). For every lineage with more than 6 lines with available expression data, Comparative Marker Selection was performed in GenePattern. The top 200 differentially overexpressed genes for each lineage compared with all other lineages were identified using a SNR. Significance testing of shRNAscores between high and low *PAX8* expressing lines was done with a *t* test (*n* = 83, mean *PAX8* expression dividing high and low classes).

Plasmids. To generate a plasmid coexpressing shRNA and GFP, a GFP cDNA fragment was cloned into the BamHI and KpnI sites of pLKO.1-puro-shRNA to replace the puromycin resistance gene. A pool of 85 control shRNAs targeting reporter genes (GFP, RFP, Luciferase, and LacZ) was used to generate control lentiviruses (Control shRNAs) (1). The sequences targeted by *PAX8*-specific shRNAs are as follows:

TRCN0000021274 (shPAX8#3: 5′-CCTTCGCCATAAAGC-AGGAAA-3′),
TRCN0000021275 (shPAX8#5: 5′-GCAACCATTCAACCT-CCCTAT-3′),
TRCN0000021276 (shPAX8#4: 5′-CTCTTTATCTAGCTCC-GCCTT-3′),
TRCN0000021277 (shPAX8#2: 5′-CCCAGTGTCAGCTCC-ATTAAT-3′)
and TRCN0000021278 (shPAX8#1: 5′-CCGACTAAGCAT-TGACTCACA-3′).

Cell Proliferation Assay. Cells were seeded into each well of 96-well plates (Costar) 24 h before infection. Six replicate infections were performed for control shRNAs and each *PAX8*-specific shRNA in the presence of 4 μg/mL polybrene for 24 h. After the incubation, medium was replaced with fresh medium with triplicates containing 2 μg/mL puromycin, and cells were cultured for 5 d. The ATP content was measured using CellTiter-Glo luminescent cell viability assay (Promega). Data represent mean + SD of six replicate infections relative to infection with control shRNAs.

Immunoblotting. Cell lysates were prepared by scraping cells in lysis buffer [50 mM Tris HCl (pH 8), 150 mM NaCl, 1% Nonidet P-40, 0.5% sodium deoxycholate, and 0.1% SDS] containing 1× Complete protease inhibitors (Roche) and phosphatase inhibitors (10 mM sodium fluoride and 5 mM sodium orthovanadate). Protein concentration was measured using BCA Protein Assay kit (Pierce). An equal amount of protein (30 μg) was separated by NuPAGE Novex Bis-Tris 4–12% gradient gels (Invitrogen) and then transferred onto a poly(vinylidene difluoride) membrane (Amersham) using a Bio-Rad electrophoretic tank blotting apparatus. The membrane was then incubated with primary antibody for 1 h at room temperature. Antibody against PAX8 (sc-81353) was purchased from Santa Cruz Biotechnology. Antibody against poly(ADP-ribose) polymerase (#9532) was purchased from Cell Signaling Technology. After incubation with the appropriate horseradish peroxidase-linked secondary antibodies (Bio-Rad), signals were visualized by enhanced chemiluminescence plus Western blotting detection reagents (Amersham). β-actin was also assessed as an internal loading control by using a specific antibody (sc-8432-HRP, Santa Cruz).

1. Luo B, et al. (2008) Highly parallel identification of essential genes in cancer cells. *Proc Natl Acad Sci USA* 105:20380–20385.
2. Thomas RK, et al. (2007) High-throughput oncogene mutation profiling in human cancer. *Nat Genet* 39:347–351.
3. Forbes SA, et al. (2008) The Catalogue of Somatic Mutations in Cancer (COSMIC). *Curr Protoc Hum Genet* 57:10.11.1–10.11.26.
4. TCGA-Network (2011) Integrated genomic analyses of ovarian carcinoma. *Nature*, in press.
5. Weir BA, et al. (2007) Characterizing the cancer genome in lung adenocarcinoma. *Nature* 450:893–898.
6. Cancer Genome Atlas Research Network (2008) Comprehensive genomic characterization defines human glioblastoma genes and core pathways. *Nature* 455:1061–1068.
7. Beroukhim R, et al. (2010) The landscape of somatic copy-number alteration across human cancers. *Nature* 463:899–905.

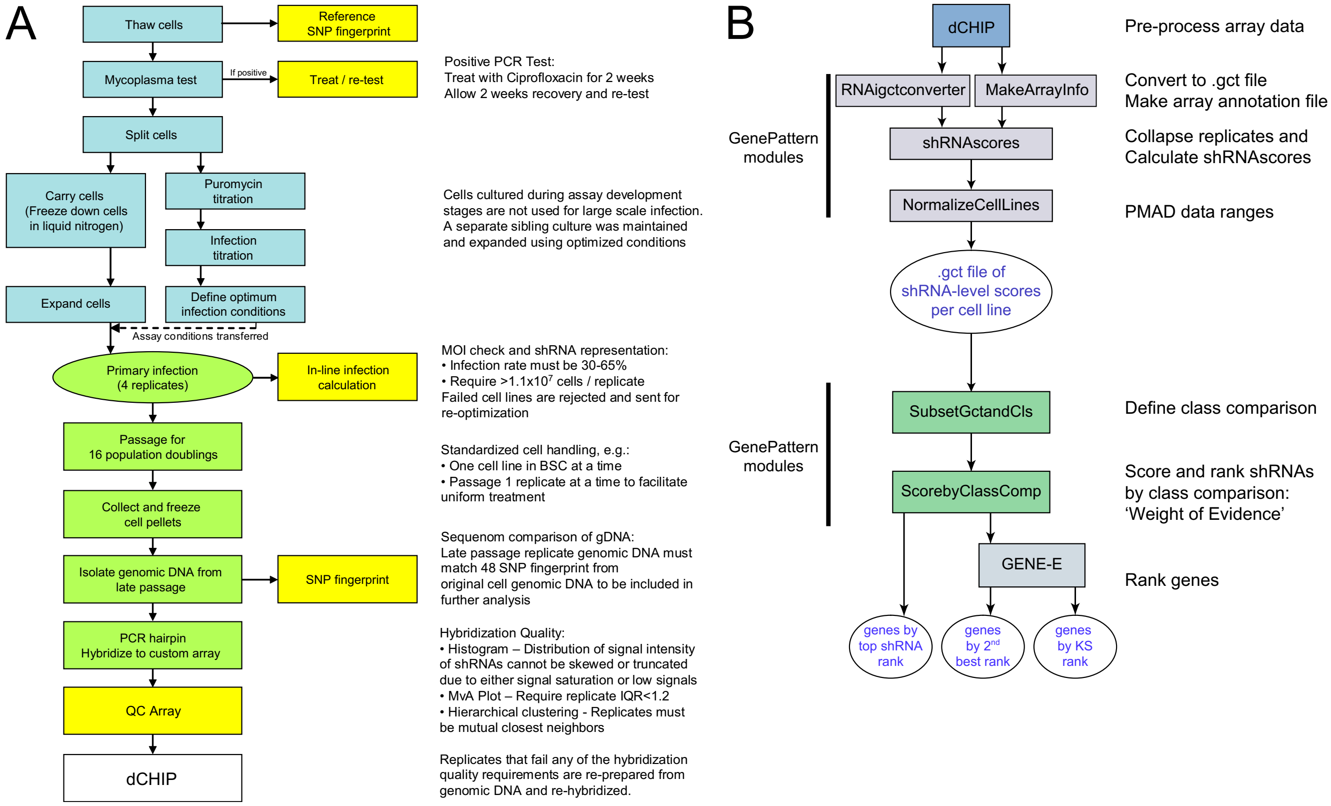
A
Thaw cells
Reference SNP fingerprint
Mycoplasma test
If positive
Treat / re-test
Split cells
Carry cells (Freeze down cells in liquid nitrogen)
Puromycin titration
Infection titration
Expand cells
Define optimum infection conditions
Assay conditions transferred
Primary infection (4 replicates)
In-line infection calculation
Passage for 16 population doublings
Collect and freeze cell pellets
Isolate genomic DNA from late passage
SNP fingerprint
PCR hairpin Hybridize to custom array
QC Array
dCHIP
B
dCHIP
RNAigctconverter
MakeArrayInfo
shRNAscores
NormalizeCellLines
GenePattern modules
.gct file of shRNA-level scores per cell line
SubsetGctandCls
ScorebyClassComp
GenePattern modules
GENE-E
genes by top shRNA rank
genes by 2nd best rank
genes by KS rank
Pre-process array data
Convert to .gct file
Make array annotation file
Collapse replicates and Calculate shRNAscores
PMAD data ranges
Define class comparison
Score and rank shRNAs by class comparison: 'Weight of Evidence'
Rank genes

Positive PCR Test:
Treat with Ciprofloxacin for 2 weeks
Allow 2 weeks recovery and re-test

Cells cultured during assay development stages are not used for large scale infection. A separate sibling culture was maintained and expanded using optimized conditions

MOI check and shRNA representation:
- Infection rate must be 30-65%
- Require >$1.1\text{x}10^7$ cells / replicate

Failed cell lines are rejected and sent for re-optimization

Standardized cell handling, e.g.:
- One cell line in BSC at a time
- Passage 1 replicate at a time to facilitate uniform treatment

Sequenom comparison of gDNA:
Late passage replicate genomic DNA must match 48 SNP fingerprint from original cell genomic DNA to be included in further analysis

Hybridization Quality:
- Histogram – Distribution of signal intensity of shRNAs cannot be skewed or truncated due to either signal saturation or low signals
- MvA Plot – Require replicate IQR<1.2
- Hierarchical clustering - Replicates must be mutual closest neighbors

Replicates that fail any of the hybridization quality requirements are re-prepared from genomic DNA and re-hybridized.

Fig. S1. Overviews of pooled screening and analytical pipelines. (*A*) We developed a streamlined, standardized process for cell line assay development (blue boxes), infection (green oval), and passaging (green boxes) to minimize variations in handling and culture conditions. Several quality control steps were implemented at different stages within the process (yellow boxes). All cell lines have a known reference 48 SNP Sequenom genotype before initiating the screen. Thawed cells were tested for the presence of mycoplasma by PCR before screening. Mycoplasma contaminated cell lines were cultured in the presence of 10 μg/mL ciprofloxacin for 2 weeks followed by 2 weeks of culture in standard growth medium. Cell lines that passed the mycoplasma PCR retest were allowed to reenter the screening pipeline. The cells used for shRNA lentiviral pool infections are parallel "sibling" cultures of those cells used for assay development. Puromycin sensitivity was determined by treating infected and uninfected cells with puromycin doses ranging from 0 to 10 μg/mL. Infection titration was performed over a range of 0–400 μL of virus per well of a 12-well plate using the same protocol as a large-scale infection (see *SI Methods* for details). After large-scale infection, an in-line measurement of infection rate was calculated by dividing the number of viable cells after puromycin selection over number of viable cells without puromycin selection. Infection rates between 30–65% were deemed acceptable for screening, and cell lines with infection rates outside this range were reoptimized. Cells were passaged for 16 population doublings or 28 d (whichever was longer) using a standardized passaging protocol. Genomic DNA from the final cell harvest was isolated, and cell line identity was confirmed by SNP genotyping and comparison with reference genotypes. Virally integrated shRNA sequences were PCR-amplified from genomic DNA, and products were hybridized to a custom microarray to determine the representation of shRNAs. The quality of the hybridization was assessed by examining probe distribution histograms. Replicate reproducibility was determined by examining both MvA plots and hierarchical clustering dendrograms. Outlier samples with respect to hybridization intensity distribution or replicate reproducibility were reevaluated starting from genomic DNA (see *SI Methods* for details). Three or four high-quality replicates were obtained for each of 102 cell lines screened. (*B*) Analysis pipeline. A schematic showing the analytic pipeline created to process pooled RNAi screening data. Raw array data (.CEL files) were first processed with a modified version of dCHIP (1). The rest of the pipeline used GenePattern modules designed to take in the dCHIP normalized array measurements ("RNAigctconverter") and produce shRNA-level data ("shRNAscores," "NormalizeCellLines"), then calculate a WoE score for each shRNA that measures a differential effect based upon a class comparison ("SubsetGctandCls," ScorebyClassComp"). The GENE-E program was used to take the ranked differential shRNAscores between two classes and collapse to gene-level data.

1. Luo B, et al. (2008) Highly parallel identification of essential genes in cancer cells. *Proc Natl Acad Sci USA* 105:20380–20385.

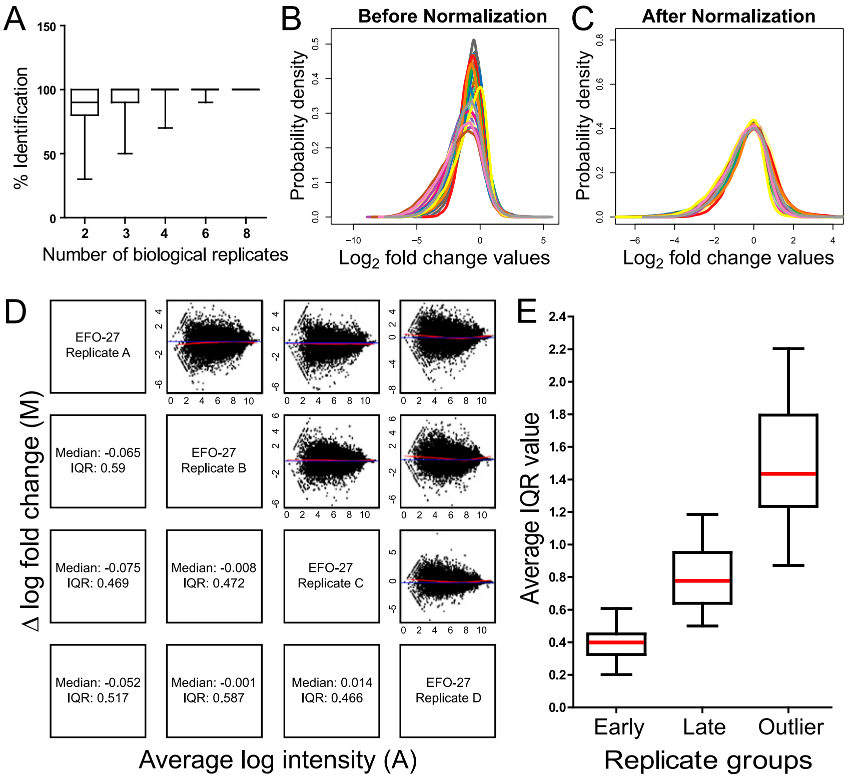

Fig. S2. Replicate number, normalization, and replicate reproducibility. (*A*) Published data (1) from 10 replicate infections of Jurkat cells were used to assess the minimum number of replicates required to generate an accurate list of shRNAscores and ranks. The log fold change of shRNA abundance in Jurkat late time point replicates relative to the initial reference plasmid DNA pool replicates were computed. The top 250 most depleted shRNAs in the 10-replicate set were identified. Randomly chosen subsets of replicates with replicate sizes of 2, 3, 4, 6, or 8 out of the 10 replicates were selected, and analysis was performed to determine the frequency at which the top 250 shRNAs from the 10-replicate set appeared within the top 1,000 ranked shRNAs in the smaller replicate set. The percent identification was averaged across the 10 subsampled datasets for each replicate size, where 100% identification indicates an ideal list identical to the list of shRNAs obtained in the 10-replicate set. The boxes represent the 25th to 75th percentile of the data, and whiskers extend to the extremes. The 4-replicate set was observed to accurately identify these top scoring constructs at high frequency. (*B* and *C*) Peak median absolute deviation (PMAD) normalization. The probability density (*y* axis) was plotted for the adjusted $\log_2$ fold change scores (*x* axis) of each cell line (colored by line) before (*B*) and after (*C*) PMAD normalization. PMAD normalization was performed by subtracting the value of each shRNA from the modeled peak value of the distribution of each cell line and dividing by the median absolute deviation of each line. (*D* and *E*) Replicate reproducibility. (*D*) MvA plots for four unnormalized replicates of EFO-27. For each pair of replicates, the difference between replicate values for $\log_2$ fold change of signal (*y* axis) is plotted against the average of $\log_2$ signal for those two replicates (*x* axis) (these plots shown in matrix positions above the diagonal). In addition, median and interquartile range (IQR) for the interreplicate differences in $\log_2$ fold change signal values are reported for each pairwise comparison (in corresponding matrix positions below the diagonal). Values for both IQR and median close to zero represent tightly clustered arrays. (*E*) The observed range of cell-line averaged IQR values across cell lines are displayed for early time point replicates (5 d postinfection), late time point replicates, and a generated set of artificial "outlier" replicates. The outlier IQR values were generated by combining three cell line replicates with a mismatched replicate from a different cell line. These artificial four-replicate sets thus model the expected distribution of IQR values in the case that one of the four chip replicates is a dramatic outlier. The red line in each box-plot is the median value for the group; boxes represent the 25th to 75th percentile of the data, and whiskers span the extremes.

1. Luo B, et al. (2008) Highly parallel identification of essential genes in cancer cells. *Proc Natl Acad Sci USA* 105:20380–20385.

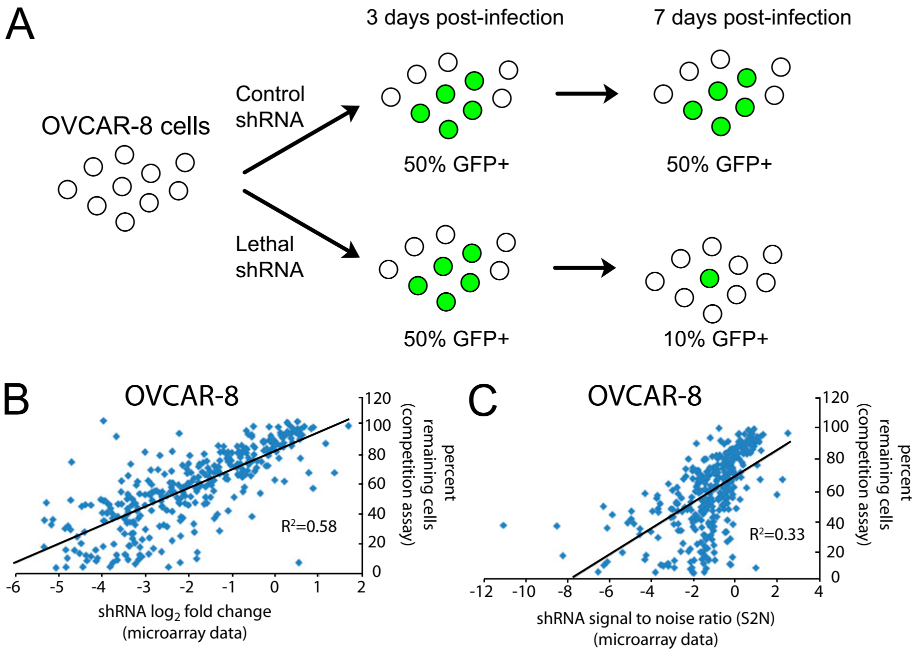

Fig. S3. Evaluation of different shRNA pooled screen scoring methods against individual shRNA proliferation tests. (*A*) Experimental schematic. OVCAR-8 cells were infected with each of the 350 shRNAs to transduce ~50% of the cells. Percentage of GFP+ cells 3 and 7 d postinfection was measured by FACS. (*B* and *C*) The relative abundance of OVCAR-8 cells infected with 350 individual shRNAs encoded in a GFP+ plasmid (*y* axis, relative to 3 d post infection) measured at 7 d post infection are plotted against the relative abundance of each shRNA in the pooled shRNA screen as quantified by different two different functions of the microarray hybridization data. Correlation plots are shown for $\log_2$ fold change (R^2 = 0.58) (*B*) and signal-to-noise ratio (R^2 = 0.33) (*C*). Based on these results, $\log_2$ fold change was selected as the basis for a shRNA scoring method for all subsequent analyses.

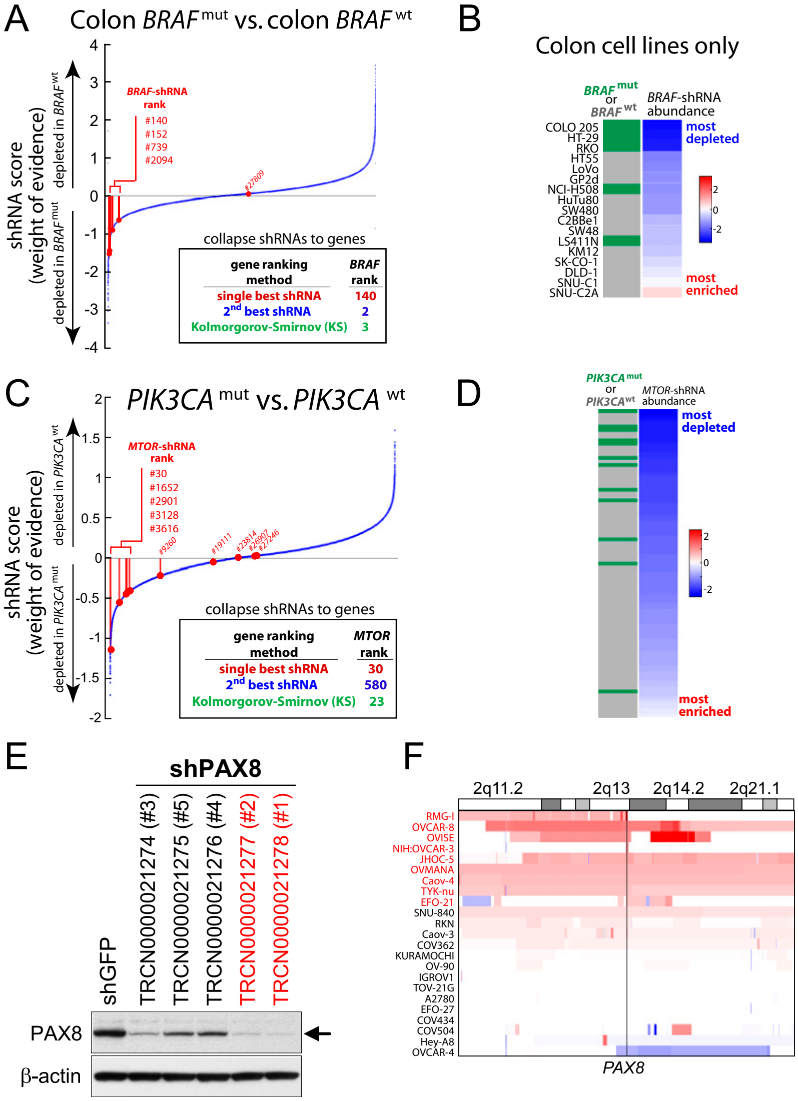

Fig. S4. Identification of essential genes in *BRAF* mutant, *PIK3CA* mutant, or 2q13-amplified cancer cell lines. (*A*) Identification of essential genes in *BRAF* mutant colon cancer cells. Distribution of shRNA ranks (*x* axis) by the WoE scores (*y* axis) for the class comparison of 5 *BRAF* mutant vs. 10 *BRAF* wild-type colon cancer cell lines only. shRNAs targeting *BRAF* are marked in red and their ranks are listed. *Inset* reports the gene ranks of *BRAF* for preferential proliferation-essentiality in the subset of cell lines with activating mutations in *BRAF*. (*B*) *BRAF*-shRNA depletion values correlate with *BRAF* mutation. Heatmap shows the fold depletion of a *BRAF*-shRNA (TRCN0000006291) in individual cell lines, sorted from most to least depleted. Mutation status is indicated in the top bar; mutant lines are in green, wild-type lines in gray. (*C* and *D*) Dependence on *MTOR* in *PIK3CA* mutant cancer cell lines. (*C*) Distribution of shRNA ranks (*x* axis) by the WoE scores (*y* axis) for the class comparisons of *PIK3CA* mutant vs. *PIK3CA* wild-type cell lines. shRNAs targeting *MTOR* are marked in red and their ranks are listed. *Inset* reports the gene rank of *MTOR* for preferential proliferation-essentiality in the subset of cell lines with activating mutations of *PIK3CA*. (*D*) *MTOR*-specific shRNA depletion values correlate with *PIK3CA* mutation status. Heatmap shows the fold depletion of the top-scoring *MTOR*-specific shRNA (TRCN0000038677) in individual cell lines, sorted from the most to least depleted. Mutation status of *PIK3CA* is indicated in the left bar; mutant lines are in green, wild-type lines in gray. (*E*) Validation of target gene suppression by *PAX8*-specific shRNAs. Immunoblot confirmed target gene suppression by top-scoring *PAX8*-specific shRNAs. OVCAR-4 cells were infected with a control shRNA targeting GFP or *PAX8*-targeting shRNAs, and cell lysates were collected 4 d after infection for immunoblotting. Two effective shRNAs, labeled in red, were further tested for their proliferation effects in a panel of ovarian cancer cell lines in Fig. 4. (*F*) Amplification of *PAX8* (2q13) in ovarian cancer cell lines. SNP array colorgram depicts genomic amplification of *PAX8*. Regions of genomic amplification and deletion are denoted in red and blue, respectively. Black vertical lines denote the boundaries of *PAX8* gene. Ovarian cancer cell lines are labeled in red if they harbor amplification of *PAX8* ($\log_2$ copy number ratio > 0.3).

Other Supporting Information Files

Table S1 (DOC)
Table S2 (DOC)
Table S3 (DOC)
Table S4 (DOC)
Table S5 (DOC)